

## Strong noncollinearity between nonequivalent Nd magnetic moments in Nd<sub>2</sub>Fe<sub>14</sub>B at low temperature

F. Bartolomé<sup>a)</sup>

*I.C.M.A., CSIC-Universidad de Zaragoza, 50009 Zaragoza, Spain, and Laboratoire de Cristallographie, C.N.R.S. BP166, 38042 Grenoble, France*

J. M. Tonnerre, N. Jaouen, and D. Raoux

*Laboratoire de Cristallographie, C.N.R.S. BP166, 38042 Grenoble, France*

J. Chaboy and L. M. García

*I.C.M.A., CSIC-Universidad de Zaragoza, 50009 Zaragoza, Spain*

H. Maruyama

*Department of Physics, Faculty of Science, Okayama University, Japan*

R. Steinmann

*European Synchrotron Radiation Facility, B.P. 220, 38043 Grenoble Cedex, France*

A temperature-dependent x-ray resonant magnetic scattering study through the spin reorientation transition (SRT) that Nd<sub>2</sub>Fe<sub>14</sub>B undergoes below  $T_{\text{SRT}}=135$  K is presented. The experimental results evidence a strong noncollinearity between the magnetic moments of Nd atoms in 4*f* and 4*g* crystallographic sites in the low-temperature phase. © 2000 American Institute of Physics. [S0021-8979(00)29608-4]

Nd<sub>2</sub>Fe<sub>14</sub>B undergoes a spin reorientation transition (SRT) below  $T_{\text{SRT}}=135$  K,<sup>1</sup> which destroys the high-temperature uniaxial anisotropy (magnetization parallel to the *c* axis). The SRT gives way to a different magnetic structure in which the easy-axis magnetization direction (EMD) rotates from the *c* axis toward the [110] direction, at a reorientation angle,  $\theta_{\text{SRT}}$ , which increases continuously by lowering the temperature below  $T_{\text{SRT}}$ . Magnetization measurements determine a macroscopic value of about 30° for  $\theta_{\text{SRT}}$  at the lowest temperatures.<sup>1,2</sup> Moreover, the magnetic moment of Nd ions increases abruptly below  $T_{\text{SRT}}$  as evidenced by <sup>57</sup>Fe and <sup>145</sup>Nd Mössbauer spectroscopy.<sup>3,4</sup>

The collinearity between the magnetic moments in Nd<sub>2</sub>Fe<sub>14</sub>B below  $T_{\text{SRT}}$  has been a subject of study and controversy for a long time.<sup>5</sup> Nd<sub>2</sub>Fe<sub>14</sub>B structure, belonging to the *P4*<sub>2</sub>/*mmn* group, presents six different crystallographic positions for Fe and two for Nd ions,<sup>5-7</sup> 4*f* and 4*g* (we will use the site notation of Ref. 1). A detailed understanding of the anisotropy and magnetic structure of Nd<sub>2</sub>Fe<sub>14</sub>B lies in the development of models treating together the crystal electric field (CEF) splitting of the Nd ions and the Nd-Fe exchange interaction. However, the derivation of a correct CEF Hamiltonian deals with the determination of nine parameters for each Nd site. Usually, a rigidly collinear structure approximation has been employed, both above and below  $T_{\text{SRT}}$ , reducing in this way the number of necessary CEF parameters.<sup>6</sup> The resulting simplified expressions (for the anisotropic energy,<sup>7</sup> for instance), are only valid in rigidly collinear situations.

The calculated low-temperature magnetic structures within these models are collinear or slightly noncollinear, with relative canting angles of at most 3° between Nd and Fe moments.<sup>6</sup> Even more, together with other simplifying (and

somehow necessary) approximations, the *f*-*g* site dependence has been neglected by a number of authors<sup>5</sup> in order to reduce the intrinsic parameter freedom of a general CEF-exchange Hamiltonian in such a complex structure.

In contrast with this general theoretical collinear or almost-collinear scenario, there has been some evidence of noncollinearity in the low temperature phase from several experimental techniques.<sup>5</sup> Recently, x-ray magnetic circular dichroism (XMCD) experiments at the Fe *K*- and Nd *L*<sub>2,3</sub>-absorption edges demonstrated the occurrence of a noncollinear arrangement between the Fe and Nd average moments below  $T_{\text{SRT}}$ .<sup>8,9</sup> Combined XMCD experiments<sup>10</sup> at the Fe *L*<sub>2,3</sub> and Nd *M*<sub>4,5</sub> absorption edges allowed us to quantitatively determine  $\theta_{\text{SRT}}^{\text{Fe}}=28^\circ$  and  $\theta_{\text{SRT}}^{\text{Nd}}=40^\circ$  at  $T=4$  K, a strong relative canting below  $T_{\text{SRT}}$ , in qualitative agreement with previous <sup>145</sup>Nd Mössbauer measurements.<sup>4</sup> In order to experimentally probe the collinearity of the Nd magnetic moments occupying 4*f* and 4*g* sites below  $T_{\text{SRT}}$ , an element- and site-specific technique such as x-ray resonant magnetic scattering (XRMS) is required. XRMS, which is the scattering counterpart of XMCD, combines the atomic selectivity of x-ray core excitation techniques with the structural information of a diffraction experiment. A previous XRMS study<sup>11</sup> suggested the possibility of a noncollinear arrangement of Nd magnetic moments at 4*f* and 4*g* sites below  $T_{\text{SRT}}$ , but that work did not reach quantitative results.

The experiments have been performed on a plate-shaped single crystal of Nd<sub>2</sub>Fe<sub>14</sub>B. The geometry of the experiment is depicted in the left panel of Fig. 1. The beam was impinging on a polished face, parallel to the [110] planes. Horizontal plane diffraction geometry was used. The incident beam (**k**, **ε**) is fully linearly polarized in the plane of the synchrotron orbit. The easy axis of the magnetization in the high-temperature ferromagnetic phase is parallel to the (001) crystal axis. A switchable applied magnetic field of 1 kOe was

<sup>a)</sup>Electronic mail: bartolom@posta.unizar.es

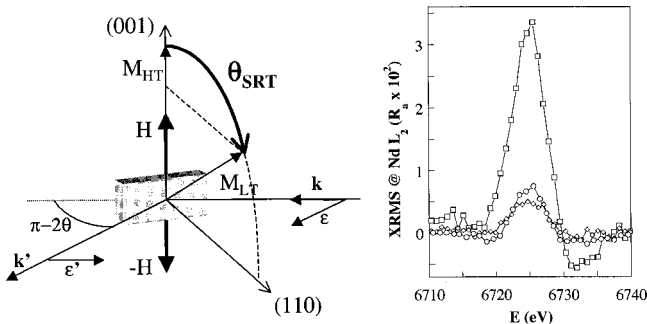


FIG. 1. Left panel: Scheme of the experimental geometry. Right panel: Room temperature XRMS  $R_a$  spectra for the (440) ( $\square$ ), (330) ( $\diamond$ ), and (220) ( $\circ$ ) Bragg reflections recorded at the Nd  $L_2$  absorption edge.

applied along the vertical (001) axis, perpendicular to the scattering plane. The experiments were carried out on the CRG-IF and ID20 beam-lines at the ESRF. To access the required temperature range, we used a ‘cold-finger’  $N_2$  cryostat, specifically designed and constructed for this experiment.<sup>12</sup>

We recorded the intensity of the scattered beam ( $\mathbf{k}'$ ,  $\boldsymbol{\epsilon}'$ ) corresponding to ( $hh0$ ) Bragg reflections upon reversal of the applied magnetic field, as a function of the incident energy for a series of temperatures above and below the SRT. The maxima of the Bragg peaks were followed along the energy spectra. To bring out the magnetic signal, the asymmetry ratio of the XRMS,  $R_a = (I^+ - I^-) / (I^+ + I^-)$ , was measured at energies near the Nd  $L_2$  absorption edge.  $I^+$  ( $I^-$ ) denote the diffracted intensity with the applied field parallel (antiparallel) to the cross product ( $\boldsymbol{\epsilon} \times \boldsymbol{\epsilon}'$ ). The  $R_a$  curves recorded at the (220), (330), and (440) Bragg reflections around the Nd  $L_2$  absorption edge at room temperature are shown in the right panel of Fig. 1.<sup>13</sup> The maxima of  $R_a$  are 0.035, 0.008, and 0.005 for the (440) ( $\square$ ), (220) ( $\circ$ ), and (330) ( $\diamond$ ) reflections, respectively, due to their different structure factors,  $F_{(hh0)} = \sum_{i=1}^N f \exp[2\pi i h(x_i + y_i)]$  where  $x_i$  and  $y_i$  are the  $ab$  plane coordinates of the  $i$ th atom within the unit cell. Lorentz and absorption corrections do not affect  $R_a$  as far as those factors affect both  $I^+$  and  $I^-$  in the same way.  $f_i$  is the atomic scattering factor,  $i = \text{Nd, Fe, and B}$ . As the incident energies are scanned near the Nd  $L_2$  absorption edge,  $f_{\text{Nd}}$  includes, in addition to the nonresonant  $f_0$ , the anomalous and the magnetic resonant terms,  $f_{\text{Nd}} = -(\boldsymbol{\epsilon} \cdot \boldsymbol{\epsilon}') \times (f_0 + f' + if'') + f_{\text{mag}}^{\text{res}}$ . Nonresonant x-ray magnetic scattering is much smaller than the resonant one near the absorption edges, and will be neglected. It has been well established that the magnetic signal observed at 6725 eV is due to dipolar  $2p \rightarrow 5d$  transitions only.<sup>14,9</sup> Thus, by neglecting quadrupolar terms, the XRMS term can be expressed as

$$f_{\text{mag}}^{\text{res}} = \frac{3}{4} \chi \{ -i(\boldsymbol{\epsilon}' \times \boldsymbol{\epsilon}) \cdot \boldsymbol{\mu}_{\text{Nd}} [F'_{11} - F'_{1-1}] + (\boldsymbol{\epsilon}' \cdot \boldsymbol{\mu}_{\text{Nd}})(\boldsymbol{\epsilon} \cdot \boldsymbol{\mu}_{\text{Nd}}) [2F'_{10} - F'_{11} - F'_{1-1}] \}, \quad (1)$$

where  $F'_{\Delta L, \Delta M}$  are the resonant responses<sup>15</sup> characterized by the order of the transition ( $\Delta L = 1$ , for dipolar terms). The prime notation indicates that we have explicitly taken out from  $F$  the dependence on  $|\boldsymbol{\mu}_{\text{Nd}}|$ , the atomic magnetic moment of Nd. Only the first term changes sign when the magnetic field is flipped, being the largest contribution to  $R_a$ .

This implies, in the present experimental geometry, that for a given Bragg reflection and incident energy, the XRMS asymmetry ratio is roughly proportional to the projection of the magnetic moments of Nd atoms on the  $c$  axis,  $\boldsymbol{\epsilon} \times \boldsymbol{\epsilon}'$  being parallel to (001). The variation of the Nd magnetic moment with temperature has been obtained<sup>3</sup> by magnetization and Mössbauer spectroscopy measurements. Then, one can obtain  $\theta_{\text{SRT}}^{\text{Nd}}$  as a function of temperature by recording a series of XRMS spectra at selected temperatures. Moreover, if the investigated Bragg reflections are conveniently chosen, the evolution of  $\theta_{\text{SRT}}^{4f}$  and  $\theta_{\text{SRT}}^{4g}$  can be almost independently regarded. For the present structure, ( $hh0$ ) reflections provide three cases of choice: the relative weight of the two sites,  $4f/4g$ , on the geometrical part of the squared structure factor,  $F^2$ , are  $2 \times 10^{-3}$ , 35.6, and 1.2, for  $h = 2, 3$ , and 4 respectively. This renders it possible to separately investigate the reorientation angles of the two  $4f$  and  $4g$  sites, by measuring the evolution of the three reflections: (330) is almost only sensitive to the projection onto the  $c$  axis of the  $4f$  magnetic moments, (220) is originated at 99.8% by  $4g$  sites, while (440) provides an averaged signal. However, to rigorously quantify the canting angles, we do calculate  $R_a$  from the intensities  $I^\pm = F_\pm^2$  using the algorithm described elsewhere,<sup>13</sup> taking into account the contributions from  $4f$  and  $4g$  Nd atoms separately. If the only important contribution comes from the dot product  $(\boldsymbol{\epsilon}' \times \boldsymbol{\epsilon}) \cdot \boldsymbol{\mu}_{\text{Nd}}$ , then the evolution of the three  $R_a$  spectra should be fully determined by using one temperature-dependent scaling factor.

Figure 2 shows selected  $R_a$  spectra measured at the (440) (left panel), (330) (central panel), and (220) (right panel) reflections, for several temperatures around  $T_{\text{SRT}}$ . Note that  $R_a$  ranges are different for the three panels. Thus, from inspection of Fig. 2, one can directly state that Nd ions occupying  $4f$  and  $4g$  sites do not reorient collinearly. The  $R_a$  at the (330) reflection nearly vanishes at 100 K all along the Nd  $L_2$  edge, while it remains clearly visible at (220) and (440) reflections. A collapse of the magnetic moment of Nd ions occupying the  $4g$  sites is ruled out by Mössbauer<sup>3,4</sup> and magnetization measurements. Thus, the observed behavior evidences a  $\theta_{\text{SRT}}^{4g}$  near to  $\pi/2$ . This is much higher than the averaged values of  $\theta_{\text{SRT}}^{\text{Nd}}$  calculated by available models.<sup>5</sup>

To quantify our results in terms of  $\theta_{\text{SRT}}^{\text{Nd}}$ , we studied the relative change of the  $R_a$  with respect to the  $T = 300$  K spectra, as shown in the left panel of Fig. 3. The variation of the Nd magnetic moment<sup>3</sup> is also shown in Fig. 3. In the following, we assume that the magnetic moment of both Nd sites remain equal. This approximation is probably not strictly fulfilled, but magnetic measurements and electronic structure calculations<sup>16</sup> do not evidence important deviations, and the changes induced in the reorientation angles should be quite small. The intrinsic separation of the  $4f$  and  $4g$  moments performed by the (330) and (220) reflections render the computation of  $\theta_{\text{SRT}}^{4f}$  and  $\theta_{\text{SRT}}^{4g}$  an easy task. The reorientation angles obtained from the (440) data are used as a double check of the procedure. The right panel in Fig. 3 shows the canting angles for both sublattices as a function of temperature, as well as for the Nd averaged moment. The latter is compared with results obtained by XMCD measurements at

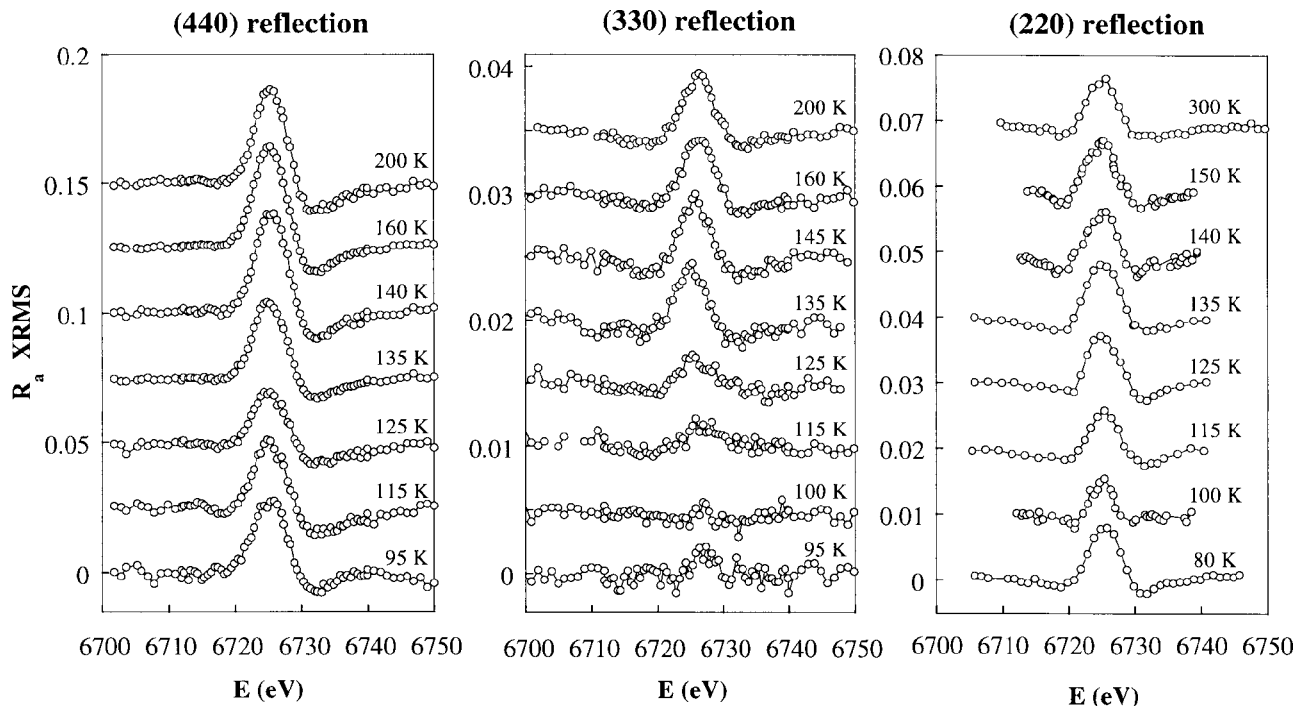


FIG. 2. X RMS  $R_a$  spectra recorded at selected temperatures and three  $(hh0)$  Bragg reflections:  $h=4$  (left), 3 (center), and 2 (right). The spectra have been shifted for the sake of clarity.

the  $M_{4,5}$  Nd edges,<sup>10</sup> which are in rather good agreement with our results.

In conclusion, our results demonstrate that a strongly noncollinear arrangement of the magnetic moments is present at low temperatures: While Nd magnetic moments occupying  $4f$  sites rotate from 140 to 100 K to  $\theta_{\text{SRT}}^{4f} \approx 80^\circ$ , the moments of Nd ions on  $4g$  sites have much smaller canting angles ( $\theta_{\text{SRT}}^{4g} \approx 25^\circ$ ). This result is in agreement with the qualitative suggestions of Koizumi and co-workers.<sup>11</sup> Finally we point out that theoretical calculations predicting (or assuming) a collinear low-temperature phase between  $4f$  and

$4g$  Nd ions and Fe must be revised as far as this point is concerned.

The authors are grateful to the staff of the CRG-IF and ID20 beamlines of the ESRF for experimental support, especially F. Rieutord, C. Vettier, and F. de Bergevin. They thank Dr. S. Sagawa from Sumitomo Special Metals Inc. for supplying the single crystal. This work has been partially supported by CICYT Project No. MAT96-0448 and the LEA-MANES CSIC-CNRS collaboration program.

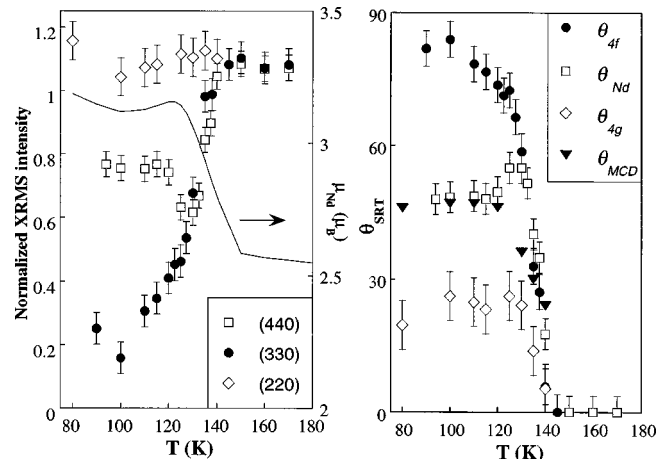


FIG. 3. Left panel: Intensity variation of X RMS (right scale) for the  $(hh0)$  reflections relative to the  $T=300$  K signal;  $h=2$  ( $\diamond$ ), 3 ( $\bullet$ ), and 4 ( $\square$ ).  $|\mu_{\text{Nd}}(T)|$  is shown as a thin line (left scale). Right panel: Reorientation angles of the  $4f$  ( $\bullet$ ),  $4g$  Nd ions ( $\diamond$ ), and Nd average reorientation angle,  $\theta_{\text{Nd}}$  ( $\square$ ). The reorientation angle obtained from XMCD ( $\blacktriangledown$ ) is also included for comparison.

<sup>1</sup>D. Givord, H. S. Li, and R. Perrier de la Bâthie, *Solid State Commun.* **51**, 857 (1984).

<sup>2</sup>K. Tokuhara, Y. Ohtsu, F. Ono, O. Yamada, M. Sagawa, and H. Yamachi, *Solid State Commun.* **56**, 333 (1985).

<sup>3</sup>H. Onoedera, H. Yamauchi, M. Yamada, H. Yamamoto, M. Sagawa, and S. Hirose, *J. Magn. Magn. Mater.* **68**, 15 (1987).

<sup>4</sup>I. Nowik, K. Muraleedharan, G. Wortmann, B. Perscheid, G. Kaindl, and N. C. Koon, *Solid State Commun.* **76**, 967 (1990).

<sup>5</sup>For a review, see J. F. Herbst, *Rev. Mod. Phys.* **63**, 819 (1991).

<sup>6</sup>J. M. Cadogan, J. P. Gavigan, D. Givord, and H. S. Li, *J. Phys. F: Met. Phys.* **18**, 779 (1988).

<sup>7</sup>M. Yamada, H. Kato, H. Yamamoto, and Y. Nakagawa, *Phys. Rev. B* **38**, 620 (1988).

<sup>8</sup>J. Chaboy *et al.*, *Phys. Rev. B* **57**, 8424 (1998).

<sup>9</sup>J. Chaboy, F. Bartolomé, L. M. García, and G. Cibin, *Phys. Rev. B* **57**, R5598 (1998).

<sup>10</sup>L. M. García, J. Chaboy, F. Bartolomé, and J. Goedkoop, *J. Appl. Phys.* (these proceedings).

<sup>11</sup>A. Koizumi, K. Namikawa, H. Maruyama, K. Mori, and H. Yamazaki, *Jpn. J. Appl. Phys., Part 2* **32**, 332 (1993).

<sup>12</sup>R. Steinmann and F. Bartolomé, *Proceedings of the Low-Temperature Physics Conference Helsinki, 1999* (electronic version).

<sup>13</sup>F. Bartolomé *et al.*, *J. Phys. IV* **7**, C2-437 (1997).

<sup>14</sup>F. Bartolomé, J. M. Tonnerre, L. Sève, D. Raoux, J. Chaboy, L. M. García, M. Krisch, and C. C. Kao, *Phys. Rev. Lett.* **79**, 3775 (1997).

<sup>15</sup>J. P. Hannon, G. T. Trammell, M. Blume, and D. Gibbs, *Phys. Rev. Lett.* **61**, 1245 (1988).

<sup>16</sup>L. Nordström, B. Johansson, and M. S. S. Brooks, *J. Phys.: Condens. Matter* **5**, 7859 (1993).